

Gibbs Free Energy of Formation of Zircon from Measurement of Solubility in H₂O

Robert C. Newton and Craig E. Manning[†]

Department of Earth and Space Sciences, University of California, Los Angeles California 90095-1567

John M. Hanchar

Department of Earth and Environmental Sciences, The George Washington University, Washington, District of Columbia 20006

Robert J. Finch

Argonne National Laboratory, Argonne, Illinois 60439

We exploited the large difference in the solubility of SiO₂ and ZrO₂ in H₂O to constrain precisely the Gibbs energy of formation of zircon (ZrSiO₄). Solubility in H₂O was determined at 800°C, 1.2 GPa, by weight loss of synthetic zircon crystals. The experiments yielded fine-grained monoclinic ZrO₂ as an incongruent solution product uniformly coating zircon crystals. Experiments on the ZrO₂-coated zircon crystals were also carried out with an initially slightly SiO₂-oversaturated fluid, causing weight gain by zircon regrowth. The mean SiO₂ concentration for forward and reverse experiments was 0.069 ± 0.010 mol/kg H₂O (2σ). When combined with precise activity–composition measurements for aqueous SiO₂, the data constrain the Gibbs free energy of zircon from its oxides at 298 K, 10⁵ Pa, to be −19.30 ± 1.16 kJ/mol (2σ). This determination is comparable in precision to the best measurements obtainable by more conventional methods, which suggests that determination of the thermochemical properties of other important ceramic materials may also be amenable to this method.

I. Introduction

BECAUSE of its durability, stability, and resistance to thermal shock, zircon is potentially useful in a wide variety of applications. However, its refractory character hinders precise determination of its Gibbs energy of formation,^{1,2} ΔG_f^o, which is required for computation of phase equilibria involving ZrSiO₄. The ΔG_f^o of zircon from the oxides



has been derived from phase-equilibrium studies^{3–5} and high-temperature oxide-melt solution calorimetry,⁶ and it is listed in compilations of thermodynamic data,^{7–9} however, values differ by over 11 kJ/mol (Table I).

Rosén and Muan³ made use of the equilibria



and



The ΔG_f^o of zircon was derived from the CO/CO₂ ratios of gases equilibrated with the solid reactants and products of the two reactions at high temperatures. Variation of ΔG_f^o with temperature is inconsistent with high-temperature heat capacity data, suggesting a systematic error, perhaps because of Co substitution in zircon.⁶ Nevertheless, a value of ΔG_f^o of zircon at 298 K, 10⁵ Pa, can be derived by combining the derived midpoint ΔG_T^o with refitted C_p functions⁶ (Table I). The apparently small uncertainty (1.16 kJ/mol, all uncertainties are 2σ unless otherwise noted) is an artifact of the narrow temperature interval over which the measurements were made (1180–1366°C).

Schuilung *et al.*⁴ used hydrothermal synthesis experiments at 1000 K, 0.1 GPa to determine the directions of several possible reactions of zircon with other minerals having reasonably well-defined thermodynamic properties. The equilibria investigated are metastable, but constraints on the Gibbs energy change of reaction 1 were obtained by determining whether the postulated reactions would or would not take place. Only broad limits on Gibbs energy change were derived, leading to a large uncertainty in ΔG_f^o of zircon (4.5 kJ/mol).

Determination of the position at high temperature (*T*) and pressure (*P*) of the univariant equilibrium



also permits derivation of ΔG_f^o of zircon. Although dependent on CO₂ equation of state and other data for the minerals, the results indicate ΔG_f^o of zircon at 298 K, 10⁵ Pa, of −18.44 ± 1.71 kJ/mol.^{5,9}

Heat of solution measurements⁶ in molten Pb₂B₂O₅ yielded a mean enthalpy of reaction 1 at 977 K of −27.90 kJ/mol. This result and refitted heat capacity data^{10–12} gave a value of ΔG_f^o at 298 K, 10⁵ Pa, of −23.57 ± 3.62 kJ/mol (Table I), where the uncertainty is the 95% confidence interval.

The phase-equilibrium and calorimetric results suggest that the Gibbs energy change of reaction 1 is between −18 and −24 kJ/mol at 298 K, 10⁵ Pa, neglecting uncertainties in individual constraints. This range only partly overlaps that given in compilations of thermodynamic data in current use for ceramic and geochemical applications^{7–9} (Table I), which rely on at least one of the above studies for free energy of formation values or imprecise estimates of the equilibrium temperature of reaction 1 at 10⁵ Pa.¹³ Sources of uncertainty in Gibbs energy of formation include experimental errors, the finite width of bracketing

L. Q. Chen—contributing editor

Manuscript No. 10118. Received April 10, 2003; approved January 12, 2005.
Supported by the Earth Sciences Division, National Science Foundation, under Grant Nos. EAR-990583 & EAR-0337170.
[†]Author to whom correspondence should be addressed. e-mail: manning@ess.ucla.edu

Table I. Summary of ΔG_f° of Zircon From the Oxides at 298 K, 10^5 Pa

ΔG_f° (kJ/mol)	2σ (kJ/mol)	Methods	Source
<i>Experiment</i>			
-20.79	1.16	High- <i>T</i> redox equilibria, 10^5 Pa, 1515–1639 K	3
-24.28	4.50	Monotropic reactions, 100 MPa, 1000 K	4
-23.57	3.62	High- <i>T</i> solution calorimetry, 10^5 Pa, 977 K	6
-18.44	1.71	High- <i>PT</i> phase equilibrium (0.7–1.1 GPa, 1073–1173 K)	5
-19.30	1.16	High- <i>PT</i> solubility, 1.2 GPa, 1073 K	This work
<i>Compilations</i>			
-13.20	—		7
-19.81	3.10		8
-17.32	3.44		9

All ΔG_f° values corrected to 298 K, 10^5 Pa, using thermal functions⁶ and expansivity and compressibility.⁹ Uncertainties reflect errors in experimental results, and ignore those in ZrO_2 and SiO_2 thermochemical data. Uncertainty for the value from Ellison and Navrotsky⁶ is the 95% confidence interval. Value from Ferry *et al.*⁵ calculated using data from Holland and Powell.⁹ Dash denotes no uncertainties given.

constraints derived from phase-equilibrium studies, and any errors in other thermochemical data used. The values in Table I omit the latter source because they were calculated using the same expansivity, compressibility, and thermal functions.^{6,9} Thus, improving the precision of phase-equilibrium determination of ΔG_f° of zircon is required to reduce the wide scatter in Table I.

Precise measurement of aqueous silica solubility at elevated *T* and *P*, by gravimetry of quenched phases or by chemical analysis of quenched fluids, yields accurate and precise free energy of formation data for the magnesian silicates.¹⁴ This method is most useful in refractory silicate systems where the other components have much lower solubilities than silica. Measurements of silica solubility of zircon, according to the dissociation reaction



should therefore, in principle, yield free energy data for reaction 1. In order to apply this method effectively, it is necessary to know accurately the activity coefficient–concentration relationship of solute silica at *T* and *P* high enough to achieve measurable solubility of zircon according to reaction 5. At low H_2O pressure, where silica solutions in equilibrium with refractory silicates are very dilute, an ideal solution approximation, in which SiO_2 activity is equal to its molar concentration, is quite adequate. At higher *P* and *T*, and consequently, higher silica solubilities, aqueous silica coexisting with refractory silicates and with quartz show substantial departure from ideal behavior, with silica activity coefficient, γ_s , progressively smaller than unity as silica mole fraction, X_s , increases. A recent experimental measurement of the γ_s – X_s relationship at 800°C and 1.2 GPa H_2O pressure over a large range of SiO_2 concentration¹⁵ makes feasible a precise determination of the free energy of formation of zircon from its oxides.

II. Experimental Procedure

Aqueous solubility measurements on synthetic zircon crystals were carried out in H_2O at 800°C and 1.2 GPa. The weight change associated with zircon dissolution and regrowth in 30–40 mg of H_2O proved to be detectable to high precision. Weight changes can be ascribed entirely to the silica solution corresponding to reaction 5 because thermodynamic calculations predict that ZrO_2 solubility is below detection at the same *P* and *T*.

We used flawless, translucent, euhedral single crystals grown by a flux-melt method using lithium molybdate (Fig. 1(a)).^{16–19} Refined lattice constants from powder X-ray diffraction are presented in Table II. The mean ZrO_2 concentration of the zircon crystals (100 analyses of random spots on zircon crystals

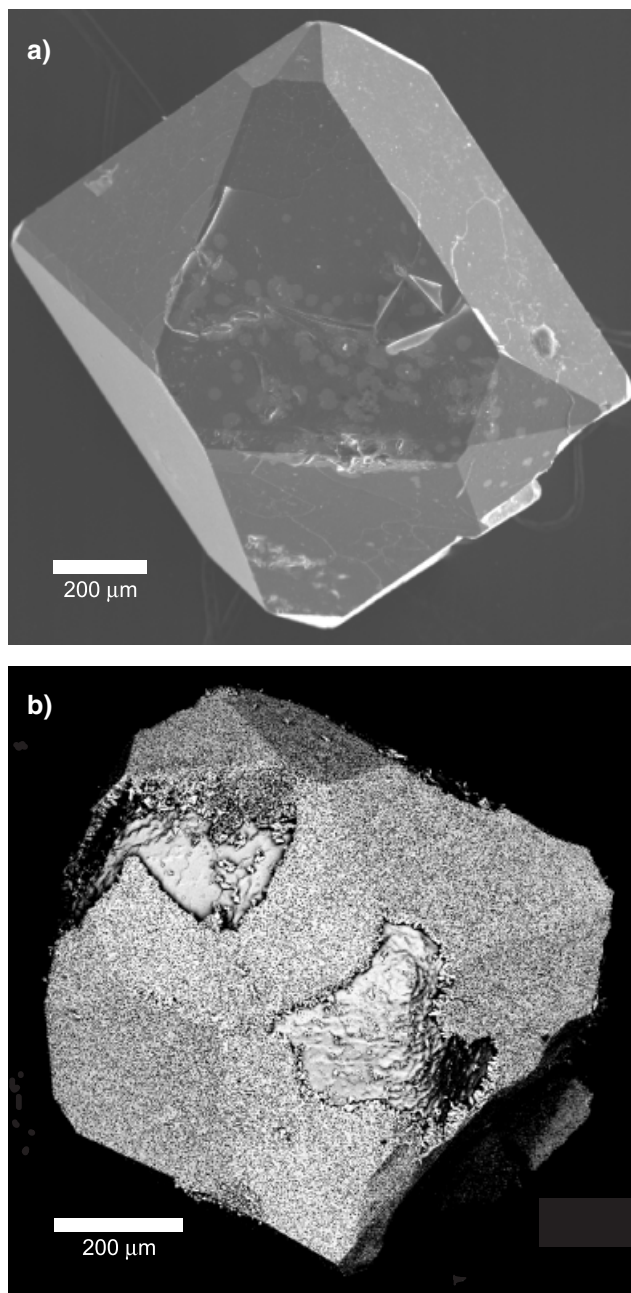


Fig. 1. Scanning-electron photomicrograph of synthetic zircon crystal (a) and baddeleyite-coated zircon (experiment #4, Table III) (b). In (b), portions of fine-grained ZrO_2 coat are broken away. Secondary electrons.

Table II. X-Ray Diffraction and Crystallographic Data for Synthetic Zircon

<i>a</i> (Å)	<i>c</i> (Å)	Volume (Å ³)	Density (g/cm ³)	Source
6.6102(8)	5.986(1)	261.57(6)	4.655	Finch <i>et al.</i> ²⁰
6.6070(1)	5.9835(1)	261.190(8)	4.660	Present study (R)
6.6078(2)	5.9831(2)	261.24(1)	4.661	Present study (P)

Errors are 1σ in last significant digit. (R) indicates results of Rietveld refinement;²¹ (P) indicates results of lattice refinement from peak-profile fits.²²

measured by electron microprobe) is 67.09% (16.65 mol% Zr), and the mean SiO₂ content is 32.79% (16.68 mol% Si). The expected stoichiometric values are 67.22% ZrO₂ (16.67 mol% Zr) and 32.78% SiO₂ (16.67 mol% Si). The small differences from the expected values are within the analytical uncertainty (0.18% RSD for Zr, 0.1% RSD for Si) of the analyses. Secondary ion mass spectrometry analyses of a randomly selected zircon crystal (*n* = 3) detected minor amounts of P (122 ppm), Li (0.12 ppm), and Mo (2.0 ppm).

Two to five zircon crystals were loaded into segments of Pt tubes of 3 mm length and 0.5 mm diameter. The tubes were lightly crimped at the ends, and some were additionally punctured with small holes to allow better access of the fluid. The small zircon-bearing capsules were sealed with about 32 mg of deionized H₂O by arc welding in a larger Pt tube segment. Runs of 70–112 h duration were made in a piston-cylinder apparatus with NaCl pressure medium and graphite heater sleeve.²³ Temperature and pressure uncertainties were, respectively, ±3°C and 0.3 kbar. At the end of each run, inner capsules were extracted and weighed. Weight losses of the inner capsules determined the solubilities. In one experiment (ZR-20), the inner capsule welded slightly to the outer capsule. In this case, solubility was determined from the weight change of the crystal itself. Weighing was carried out on a Mettler M3 microbalance, with 1σ = 2 μg. The precise determination of weight changes at the microgram level propagates to tight constraints on thermochemical properties.

III. Results

Results are given in Table III. After experiments, the zircon crystals had a tightly adhering layer of fine-grained baddeleyite, but retained their original tetragonal crystal morphology (Fig. 1(b)). Reversal experiments (ZR-11, ZR-14) were performed by reloading the baddeleyite-coated zircons from experiments ZR-4 and ZR-12 (Table III) in an inner Pt capsule, which was sealed with H₂O and a small quartz crystal into an outer Pt container. The weight of the quartz crystal was chosen so that the fluid was initially slightly silica oversaturated with respect to zircon, as determined by the forward solubility experiments. Quartz dissolution is rapid (<2 h) compared with that of refractory silicates;²⁴ this assures that a state of silica oversaturation initially prevailed. The reversal experiments yielded patchy resorption of the baddeleyite layer, with weight gains consistent with zircon regrowth.

Table III. Experimental Results, 800°C, 1.2 GPa

Experiment no.	Starting material	Time (h)	Wt H ₂ O (mg)	Start wt [†] (mg)	Extra Q (mg)	End wt [†] (mg)	<i>m</i> _{SiO₂} (mol/kg)	10 ³ <i>X</i> _{SiO₂}	Reaction direction [‡]
ZR-4	Z	109	32.967	70.303		70.185	0.060(1)	1.08(2)	↑
ZR-11	ZBQ	110	32.676	66.027	0.172	66.065	0.068(2)	1.22(4)	↓
ZR-12	Z	112	32.877	68.030		67.899	0.066(1)	1.19(2)	↑
ZR-14	ZBQ	112	33.157	69.154	0.188	69.196	0.073(2)	1.31(4)	↓
ZR-17	ZQ	88	32.775	66.533	0.085	66.483	0.069(2)	1.24(4)	↑
ZR-18	Z	70	34.056	66.432		66.289	0.070(1)	1.26(2)	↑
ZR-20	ZQ	72	32.768	2.605	0.042	2.500	0.075(2)	1.35(4)	↑

B, baddeleyite; Q, quartz (single crystal, in outer capsule); Z, zircon. [†]All start and end weights are capsule+charge except ZR-20, in which the zircon crystal was weighed directly. Parenthetical numbers are uncertainties in last significant figure from 1σ weighing uncertainties (2 μg). [‡]Downward-pointing and upward-pointing arrows denote equilibrium approached from high and low concentration, respectively.

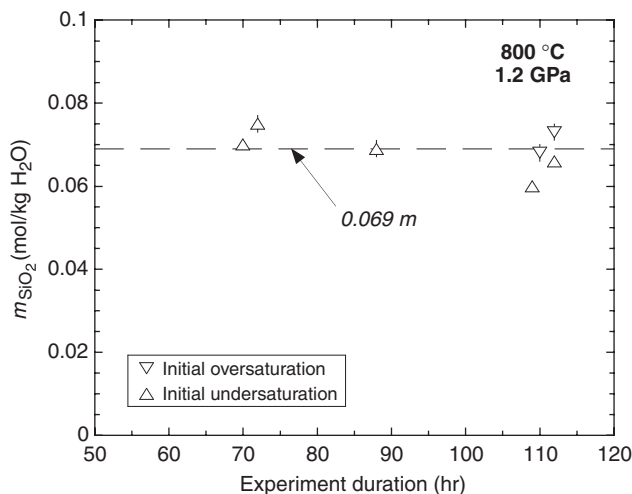


Fig. 2. SiO₂ molalities in the presence of zircon and baddeleyite at 800°C, 1.2 GPa, as a function of run duration. Upward and downward pointing triangles denote approach to equilibrium from initial under- and supersaturation (see text). Mean of six measurements (0.069 molal) shown with dashed line.

Runs of ≥70 h were sufficient to achieve equilibrium SiO₂ solute concentrations coexisting with zircon and baddeleyite (reaction 5), as indicated by the close approach of measured weight changes from opposite directions (Fig. 2). No crystalline residues were observed in the outer capsules, assuring no leakage of particulate matter, and that there was no vapor transport and regrowth of crystals of zircon or baddeleyite that could compromise the weight loss data. The only visible residues were transparent films of isotropic material inferred to be a quenched gel of SiO₂ and H₂O. The mean SiO₂ molality and mole fraction are, respectively, 0.069 ± 0.010 and 0.00143 ± 0.00019. The 2σ errors in the means of seven experiments are larger than those for individual runs because the latter account only for weighing uncertainty.

IV. Discussion

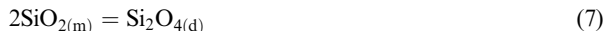
(1) Derivation of Δ*G*_f^o of Zircon at 298 K, 10⁵ Pa, from Solubility Measurements

The Gibbs free energy change of reaction 1 at a fixed *P* and *T* is given from solubility measurements by

$$\Delta G_{(1)}^o = RT \ln \left(\frac{a_s^{ZB}}{a_s^Q} \right) = RT \ln \left(\frac{\gamma_s^{ZB} X_s^{ZB}}{\gamma_s^Q X_s^Q} \right) \quad (6)$$

where *a*_s, γ_s and *X*_s are the activity, activity coefficient, and mole fraction of total dissolved silica corresponding to zircon–baddeleyite (ZB) or quartz (Q) equilibrium. The activity coefficients account for polymerization of aqueous silica.^{15,24–27} A quantitative activity model has been experimentally calibrated for

homogeneous equilibrium among aqueous silica monomers (m) and dimers (d) in the fluid phase¹⁵



Adopting a standard state for SiO_2 , total of unit activity of the hypothetical solution of unit mole fraction of monomers and a reference state of infinite dilution, and assuming an ideal solution of monomers and dimers with H_2O , the equilibrium constant, K , for Eq. (7) is

$$K = \frac{X_d}{X_m^2} \quad (8)$$

where X_d and X_m are the mole fraction of total dissolved silica occurring, respectively, as dimers and monomers, and mass balance requires that $X_s = X_m + 2X_d$. Equation (8) assumes that non-ideality of solute SiO_2 results entirely from the formation of dimers. This leads to

$$\gamma_s^B = \frac{-1 + (1 + 8KX_s^B)^{1/2}}{4KX_s^B} \quad (9)$$

where B denotes the ZB or quartz (Q) silica-activity buffers. For a given value of K (i.e., a fixed P and T), Eq. (9) describes the relationship between γ_s^B and X_s^B from $X_s^B = 0$ to quartz saturation.¹⁵ Under the conditions of the present experiments (800°C, 1.2 GPa), $K = 116\text{--}180$ (Newton and Manning¹⁵), with equal probability of any value within this range. This is in excellent agreement with $K = 129 \pm 29$ from *in situ* Raman spectroscopy at the same P and T .²⁵ Solving Eq. (9) using the midpoint of $K = 148$ and $X_s^Q = 0.0248$ from Newton and Manning¹⁵ gives $\gamma_s^Q = 0.307 \pm 0.028$. Similarly, X_s^{ZB} measured in the present study yields $\gamma_s^{\text{ZB}} = 0.778 \pm 0.008$ (Fig. 3).

Evaluation of Eq. (6) yields $\Delta G_{(1)}^\circ$ at 1.2 GPa, 1073 K, of -18.47 ± 1.16 kJ/mol. Volume, expansivity, and compressibility data⁹ and thermal functions⁶ give ΔG_f° of zircon from the oxides at 298 K, 10^5 Pa, of -19.30 ± 1.16 kJ/mol, where uncertainty from the thermophysical parameters is ignored.

(2) Comparison with Previous Estimates

Comparison of the present value of the free energy of formation of zircon with previous estimates based on experiments is given in Table I. Rosén and Muan³ derived high- T $\Delta G_{(1)}^\circ$ values, with an estimated “accuracy of ± 0.1 kcal.” However, the variation in $\Delta G_{(1)}^\circ$ with T implies heat content and entropy of reaction 1 that is inconsistent with other data.⁶ To circumvent this problem, $\Delta G_{(1)}^\circ$ was taken to be the midpoint of the reported range (at 1273°C), and it was assumed that there is uniform distribution of possible $\Delta G_{(1)}^\circ$ between the minimum and maximum values associated with the full T range (1180°–1366°C). This yields 298 K, 10^5 Pa, $\Delta G_{(1)}^\circ = -20.79 \pm 1.16$ kJ/mol (Table I). The estimate of uncertainty is higher than that for individual measurements because the data set is treated as a single constraint to account for the entropy discrepancy. However, 2σ of 1.16 kJ/mol is an artifact of the narrow T interval of the original experiments; it would be larger if the T range had been larger assuming the same trend in the data. It is also possible that there was Co substitution in zircon,⁶ which would raise additional accuracy concerns.

Schuling *et al.*⁴ derived a wide bracket on $\Delta G_{(1)}^\circ$ at 0.1 GPa, 1000 K. Correction to 10^5 Pa, 298 K, using equations and data for volume change⁹ and thermal functions⁶ gives -24.28 ± 4.49 kJ/mol. The 2σ uncertainty reflects equal probability of $\Delta G_{(1)}^\circ$ within the bracket, but this uncertainty should be considered a minimum because uncertainties in the thermodynamic properties of phases participating in the studied equilibria were not included. The experimental study⁵ of reaction 4 can be used in conjunction with data from Holland and Powell⁹ to calculate $\Delta G_{(1)}^\circ = -18.44 \pm 1.71$ kJ/mol (Table I). As above, the 2σ reflects only the width of the experimental bracket; it does not take

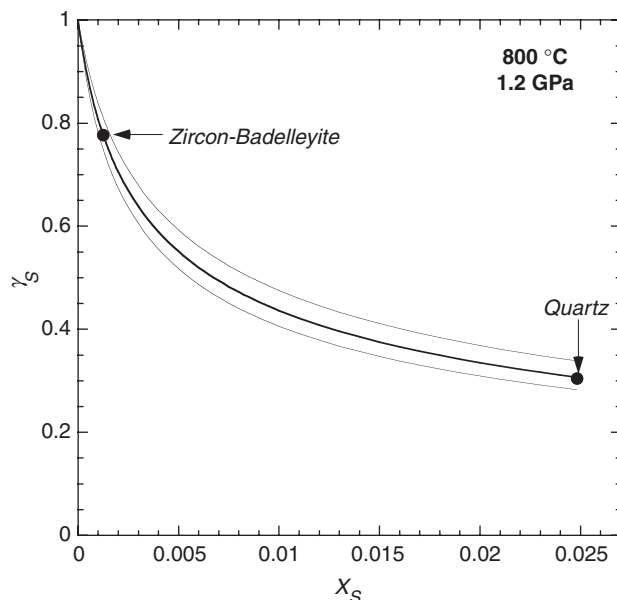


Fig. 3. Activity coefficient of aqueous silica (γ_s) from Eq. (9), text, as a function of mole fraction of aqueous silica (X_s). The bold curve was calculated using $K = 148$; the thin curves correspond to 2σ in K of 32 (Newton and Manning¹⁵). Values of γ_s are shown for experimentally determined X_s in equilibrium with quartz and zircon-baddeleyite.

into account uncertainties in thermodynamic properties of additional phases. Finally, Ellison and Navrotsky⁶ give $\Delta G_{(1)}^\circ = -23.57$ kJ/mol at 298 K, 10^5 Pa. Based on six measurements of enthalpy of solution, they report a 95% confidence interval of ± 3.62 kJ/mol.

Table I shows that the newly derived ΔG_f° of zircon from the oxides of -19.30 ± 1.16 kJ/mol is at the low end of the values derived from previous studies. It is most consistent with the result of Ferry *et al.*⁵ More significantly, comparison of uncertainties due strictly to experimental determinations (Table I) shows that the present result has a precision equal to the best previously obtained.³ Because the uncertainty in that value is probably underestimated because of the narrow T range of measurement, the present result can be considered the most precise determination to date.

Table I also lists standard free energy of formation data for zircon from its oxides at 298 K, 10^5 Pa, from several compilations of thermochemical data. Of these estimates, that of Chase *et al.*⁷ is clearly significantly less negative than, and inconsistent with, the present result, and all previous experimental studies.⁶ The reason for the systematically less negative value in the other data sets, as compared with early experimental studies, is not clear. Holland and Powell⁹ cite Robie and Hemingway,⁸ who in turn cite Schuling *et al.*⁴ and Ellison and Navrotsky⁶ as sources for the Gibbs energy of formation of zircon. Given the large uncertainties in these latter studies, the agreement must be at least in part fortuitous.

V. Applications

Solubility measurements at high P and T have proven feasible for determining the free energy of formation of a refractory silicate because of the great increase in silica solubility with pressure above 0.5 GPa H_2O pressure. The greatest challenge in refining this method as a general tool will be a more accurate definition of the activity coefficient of solute silica over a broad range of temperature and pressure. This may be achieved through detailed solubility studies on other silica-buffering assemblages, such as kyanite (Al_2SiO_5)–corundum (Al_2O_3) and rutile (TiO_2)–forsterite (Mg_2SiO_4)–geikielite (MgTiO_3).¹⁵

Other refractory silicates whose free energies of formation are at present poorly known could be studied by methods of the present study. Examples include titanite (CaTiSiO_5) with perovskite (CaTiO_3), cordierite ($\text{Mg}_2\text{Al}_4\text{Si}_5\text{O}_{18}$) with spinel (MgAl_2O_4), and sillimanite (Al_2SiO_5) with corundum. The last two systems offer the possibility of studying the effects on free energy of Al–Si order–disorder. It is possible that the degree of metamict structural degradation in natural zircon from α recoil, which is an important quantity for interpretation of geochronologic data, could be addressed by determining the solubility difference between damaged and undamaged zircon crystals, in conjunction with structural study.^{28,29}

Acknowledgments

We thank George Jarzebinski for assistance with SEM imaging, and John Ferry for discussions on zircon equilibria.

References

- ¹M. P. Tole, "The Kinetics of Dissolution of Zircon (ZrSiO_4)," *Geochim. Cosmochim. Acta*, **49** [2] 453–8 (1985).
- ²J. C. Ayers and E. B. Watson, "Solubility of Apatite, Monazite, Zircon, and Rutile in Supercritical Aqueous Fluids with Implications for Subduction Zone Geochemistry," *Philos. Trans. Roy. Soc. London, Phys. Sci. Eng.*, **335** [1638] 365–7 (1991).
- ³E. Rosén and A. Muan, "Stability of Zircon in the Temperature Range 1180° to 1366°C," *J. Am. Ceram. Soc.*, **48** [11] 603–4 (1965).
- ⁴R. D. Schuiling, L. Vergouwen, and H. Van der Rijst, "Gibbs Energies of Formation of Zircon (ZrSiO_4), Thorite (ThSiO_4), and Phenacite (Be_2SiO_4)," *Am. Mineral.*, **61** [1–2] 166–8 (1976).
- ⁵J. M. Ferry, R. C. Newton, and C. E. Manning, "Experimental Determination of the Equilibria: Rutile+Magnesite = Geikielite+ CO_2 and Zircon+2 Magnesite = Baddeleyite+2 CO_2 ," *Am. Mineral.*, **87** [10] 1342–50 (2002).
- ⁶A. J. G. Ellison and A. Navrotsky, "Enthalpy of Formation of Zircon," *J. Am. Ceram. Soc.*, **75** [6] 1430–3 (1992).
- ⁷M. W. Chase Jr., C. A. Davies, J. R. Downey Jr., D. J. Frurip, R. A. McDonald, and A. M. Syverud, "Janaf Thermochemical Tables, 3rd Edition," *J. Phys. Chem. Ref. Data*, **14** (Suppl. 1) 1–1856 (1985).
- ⁸R. A. Robie and B. S. Hemingway, "Thermodynamic Properties of Minerals and Related Substances at 298.15 K and 1 bar (10^5 Pascals) Pressure and at Higher Temperatures," *U.S. Geol. Surv. Bull.*, **2131**, 1–461 (1995).
- ⁹T. J. B. Holland and R. Powell, "An Internally Consistent Data Set for Phases of Petrologic Interest," *J. Metamorph. Geol.*, **16** [3] 309–43 (1998).
- ¹⁰K. K. Kelley, "Specific Heat of Zirconium Dioxide at Low Temperatures," *Ind. Eng. Chem.*, **36** [4] 377 (1944).
- ¹¹K. K. Kelley, "The Specific Heats at Low Temperatures of Ferrous Silicate, Manganous Silicate, and Zirconium Silicate," *J. Am. Chem. Soc.*, **63** [10] 2750–2 (1941).
- ¹²J. P. Coughlin and E. G. King, "High-Temperature Heat Contents of Some Zirconium-Containing Substances," *J. Am. Chem. Soc.*, **72** [5] 2262–5 (1950).
- ¹³C. E. Curtis and H. G. Sowman, "Investigation of the Thermal Dissociation, Reassociation, and Synthesis of Zircon," *J. Am. Ceram. Soc.*, **36** [6] 190–8 (1953).
- ¹⁴J. J. Hemley, J. W. Montoya, C. L. Christ, and P. B. Hostetler, "Mineral Equilibria in the $\text{MgO-SiO}_2\text{-H}_2\text{O}$ System: I. Talc–Chrysotile–Forsterite–Brucite Stability Relations," *Am. J. Sci.*, **277** [3] 322–51 (1977).
- ¹⁵R. C. Newton and C. E. Manning, "Activity Coefficient and Polymerization of Aqueous Silica at 800°C, 12 kbar, from Solubility Measurements on SiO_2 -Buffering Mineral Assemblages," *Contrib. Mineral. Petrol.*, **146** [2] 135–43 (2003).
- ¹⁶H. Espig, "Die Synthese des Smaragds," *Chem. Technol.*, **12** [6] 327–31 (1960).
- ¹⁷A. A. Ballman and R. A. Laudise, "Crystallization and Solubility of Zircon and Phenacite in Certain Molten Salts," *J. Am. Ceram. Soc.*, **48** [3] 130–3 (1965).
- ¹⁸A. B. Chase and J. A. Osmer, "Growth and Preferential Doping of Zircon and Thorite," *J. Electrochem. Soc.*, **113** [2] 198–9 (1966).
- ¹⁹J. M. Hanchar, R. J. Finch, P. W. O. Hoskin, E. B. Watson, D. J. Cherniak, and A. N. Mariano, "Rare Earth Elements in Synthetic Zircon. 1. Synthesis and Rare Earth Element and Phosphorus Doping," *Am. Mineral.*, **86** [5–6] 667–80 (2001).
- ²⁰R. J. Finch, J. M. Hanchar, P. W. O. Hoskin, and P. C. Burns, "Rare Earth Elements in Synthetic Zircon. 2. A Single Crystal X-Ray Study of Xenotime Substitution," *Am. Mineral.*, **86** [5–6] 681–90 (2001).
- ²¹R. A. Young, "DBWS-9411: An Upgrade of the DBWS Programs for Rietveld Refinement with PC and Mainframe Computers," *J. Appl. Cryst.*, **28** [3] 366–7 (1995).
- ²²MDI, *Jade XRD Pattern Processing Software, Version 5.0*. Materials Data, Inc., Livermore, CA, 1999.
- ²³R. C. Newton and C. E. Manning, "Quartz Solubility in $\text{H}_2\text{O-NaCl}$ and $\text{H}_2\text{O-CO}_2$ Solutions at Deep Crust-Upper Mantle Pressures and Temperatures: 2–15 kbar and 500–900°C," *Geochim. Cosmochim. Acta*, **64** [17] 2993–3005 (2000).
- ²⁴R. C. Newton and C. E. Manning, "Solubility of Enstatite+Forsterite in H_2O at Deep Crust/Upper Mantle Conditions: 4–15 kbar and 700–900°C," *Geochim. Cosmochim. Acta*, **66** [23] 4165–76 (2002).
- ²⁵Y.-G. Zhang and J. D. Frantz, "Enstatite–Forsterite–Water Equilibria at Elevated Temperatures and Pressures," *Am. Mineral.*, **85** [7–8] 918–25 (2000).
- ²⁶N. Zotov and H. Keppler, "In-Situ Raman Spectra of Dissolved Silica Species in Aqueous Fluids to 900°C and 14 kbar," *Am. Mineral.*, **85** [3–4] 600–3 (2000).
- ²⁷N. Zotov and H. Keppler, "Silica Speciation in Aqueous Fluids at High Pressures and High Temperatures," *Chem. Geol.*, **184** [1–2] 71–82 (2002).
- ²⁸L. Nasdala, M. Wenzel, G. Vavra, G. Irmer, T. Wenzel, and B. Kober, "Metamictization of Natural Zircon: Accumulation Versus Thermal Annealing of Radioactivity-Induced Damage," *Contrib. Mineral. Petrol.*, **141** [2] 125–44 (2001).
- ²⁹A. Meldrum, S. J. Zinkle, L. A. Boatner, and R. C. Ewing, "A Transient Liquid-Like Phase in the Displacement Cascades of Zircon, Hafnium, and Thorite," *Nature*, **395** [6697] 56–8 (1998). □